

Purified Dissipative Solitons With a Rectangle Spectrum From a Hybrid Mode-Locked Fiber Laser

Xing Li, Miaoqiao Wu, Weiwen Zou, *Senior Member, IEEE*, and Shixun Dai

Abstract—We demonstrate a hybrid mode-locking erbium-doped fiber laser, which combines saturable absorption and nonlinear polarization evolution. The laser is operated in the large normal dispersion regime, offering rectangle spectrum and purified femtosecond pulses with a repetition rate of 3.05 MHz and an average output power of 50.31 mW. The single-pulse energy is 16.5 nJ and the pulse peak power is 26.1 kW, providing a robust ultrafast fiber laser well suited for frequency comb generations and high-power applications.

Index Terms—Fiber laser, hybrid mode-locking, ultrafast, rectangle spectrum, purified pulse.

I. INTRODUCTION

ULTRAFAST fiber lasers have attracted much interest due to their significant advantages of excellent stability, low cost, easy operation, and compact designs. Especially, mode-locked fiber lasers with high pulse energy provide fascinating tools in various applications, including micromachining, surgical medicine, imaging, optical telecommunications, etc. Tremendous progress has been made in increasing pulse energy from fiber lasers within the past decades, and these lasers become promising candidates for competing with their solid-state counterparts [1]–[3].

The mode-locked pulse characteristics are generally determined by the interaction of dispersion and nonlinear effects. By changing the net cavity group velocity dispersion (GVD) from anomalous to normal, conventional solitons, dispersion-managed solitons, similaritons and dissipative solitons (DSs) have been achieved [4]–[7]. However, the pulse energy of the conventional solitons and dispersion-managed solitons are limited to hundreds of pJ or few nJ due to the excessive nonlinear phase shift existing in the fibers which leads to optical wave breaking or multiple pulses operation [8]. Pulses

Manuscript received June 13, 2017; revised July 12, 2017; accepted July 31, 2017. Date of publication August 16, 2017; date of current version August 29, 2017. This work is supported in part by the National Natural Science Foundation of China under Grant 61605096, Grant 61627815, Grant 61571292, and Grant 61535006, in part by the Natural Science Foundation of Ningbo under Grant 2016A610062, in part by the Opened Fund of State Key Laboratory of Advanced Optical Communication Systems and Networks under Grant 2017GZKF16, in part by the Open Fund of the Guangdong Engineering Technology Research and Development Center of Special Optical Fiber Materials and Devices under Grant 2016-3, and in part by the K. C. Wong Magna Fund in Ningbo University. (*Corresponding author: Xing Li*)

X. Li, M. Wu, and S. Dai are with the Laboratory of Infrared Materials and Devices, The Research Institute of Advanced Technologies, Ningbo University, Ningbo 315211, China (e-mail: lixing1@nbu.edu.cn).

W. Zou is with the State Key Laboratory of Advanced Optical Communication Systems and Networks, Department of Electronic Engineering, Shanghai JiaoTong University, Shanghai 200240, China.

Color versions of one or more of the figures in this letter are available online at <http://ieeexplore.ieee.org>.

Digital Object Identifier 10.1109/LPT.2017.2740718

with 3.5 nJ pulse energies and 70 fs pulse duration were achieved by the all-normal-dispersion similariton laser [9]. The dissipative solitons rely on a balance of group velocity dispersion, self-phase-modulation, saturable absorption, and spectral filtering. They have much higher energy than the other three kinds of solitons owing to strong pulse chirps resulted from large normal dispersion, thereby effectively avoiding optical wave breaking caused by the nonlinear effects. The self-consistency of the pulse is achieved by amplitude modulation namely by the saturable absorber mechanism and the spectral filtering. The DSs have been studied extensively around the wavelength of 1 μm region, at which the GVD is normal in single-mode fiber and the gain medium is suitable for producing high-energy DSs [10]–[14].

Actually, DS fiber lasers have also been realized at wavelengths around 1.55 μm with erbium-doped (Er-doped) fiber as the gain medium [15]–[23]. Chichkov *et al.* [15] demonstrated output pulse energies of 20 nJ and peak power of 16.9 kW from an all normal dispersion Er-doped fiber laser which was mode-locked using nonlinear polarization evolution (NPE) and was stabilized with a birefringent filter. Tang *et al.* [17] obtained pulse energies of 38 nJ from a resonant saturable absorber mirror based Er-doped fiber laser, which was stabilized by the combined actions of a high nonlinearity amplitude modulator and a narrow-band spectral filter. In fact, Er-doped fiber lasers with large normal dispersion can even generate high-energy DSs without using an additional spectral filter inside the cavity. The reason is that the Er-doped gain fibers have narrow gain bandwidth which functions as an effective spectral filter in the cavity. For example, Ruehl *et al.* [18] showed an Er-doped fiber laser mode-locked by NPE operating in the large normal dispersion regime. The laser produced highly chirped DSs with a pulse energy of 10 nJ and peak power of 140 kW. Liu *et al.* [19] reported an all-fiber Er-doped fiber laser mode-locked by NPE, which produced DSs with a pulse energy of 8 nJ and a pulse duration of 290 fs. Also with this schematic, C. Ouyang *et al.* [20] demonstrated a high energy Er-doped fiber laser which generated DSs with pulse energies of 12 nJ and peak power of 33 kW.

However, in the aforementioned high energy fiber lasers, the optical spectra of the DSs have two drawbacks. Firstly, they appear non-flat since several peaks existing [15], [17], [19]–[23], which present an M-shape [17], [23] or a cat-ear profile [16], or have modulation instability-induced sidebands [21]; Secondly, the spectrum pedestals can also be observed in most lasers [17], [19]–[23]. The two drawbacks lead to pedestal beats or satellite pulses existing on both sides of the compressed pulses [15], [17], [19]–[23]. These pedestal beats or satellite pulses give rise to a significant leak of pulse energy from the main peak, resulting in a

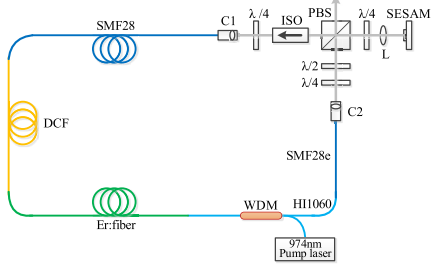


Fig. 1. Configuration of the hybrid mode-locking fiber laser with large net normal dispersion. PBS, polarization beam splitter; ISO, isolator; $\lambda/2$, half waveplate; $\lambda/4$, quarter waveplate; L, aspheric lens; WDM, wavelength-division multiplexer, C1 and C2, fiber collimator.

decrease of the pulse peak power. In this letter, we demonstrate a hybrid scheme of Er-doped mode-locked fiber laser that incorporates the NPE and semiconductor saturable absorber mirror (SESAM). Within the cavity, there is no additional spectral filter used for stabilizing the mode-locking. A segment of dispersion compensation fiber (DCF) is used to provide normal dispersion to make the laser operate in the large normal dispersion regime. The NPE is intended to shape rectangular spectrum and ultrashort pulses while the SESAM adopted here enables self-starting and suppress the temporal beat pedestals. The incorporation of these two mode-locking mechanisms results in a rectangle spectrum and purified femtosecond pulses with a spectral width of 11.2 nm and a pulse duration of 514 fs. The single-pulse energy is 16.5 nJ and the pulse peak power is 26.1 kW. This compact laser source may find its position in high-power applications, such as micromachining and laser surgery.

II. PRINCIPLE AND EXPERIMENTAL SETUP

Figure 1 depicts the sigma configuration of the hybrid mode-locking fiber laser. It is organized by a set of fibers and free-space bulk components. The fibers are composed of a highly Er-doped gain fiber (Liekki ER110-4/125), a SMF28e fiber, a long segment of DCF fiber, an OFS-980 fiber pigtail of a 980 nm/1550 nm wavelength division multiplexer (WDM), two leading fibers (SMF28e) of the fiber collimator (C1 and C2). The SMF28e fiber and DCF are employed within the cavity to increase the cavity length which decreases the repetition rate of the mode-locking pulses. The DCF is also used to increase the cavity dispersion, which leads to strong chirps of the DSs. The free-space bulk components consist of a polarization beam splitter (PBS), a half waveplate, three quarter waveplates, a polarization-dependent isolator, an aspheric lens and a SESAM (BATOP GmbH). The SESAM presents a modulation depth of 6%, a recovery time of 2 ps, and a saturation fluence of $50 \mu\text{J}/\text{cm}^2$. The PBS acts both as the polarizer for the NPE mode locking and as the laser output coupler. The quarter waveplate in the linear arm is employed for the vertical-to-horizontal polarization rotation, which ensures high-efficiency pass through the PBS. The aspheric lens is used to focus the beam (focal length = 11 mm) onto the SESAM. The isolator is inserted after the PBS to allow unidirectional operation within the cavity. The long segment DCF and SMF28e fiber are located after the output coupler where optical power is weak to reduce the cumulative nonlinear phase shift. The gain fiber is

TABLE I
PARAMETERS OF ALL FIBERS IN THE HYBRID MODE-LOCKING FIBER LASER

	Er:fiber	SMF28e	DCF	HII060	SMF28e (C1)	SMF28e (C2)
Length (m)	0.4	26.1	38.15	0.35	0.15	0.15
GVD (fs^2/mm)	11.9	-21.7	48.4	-10.8	-21.7	-21.7

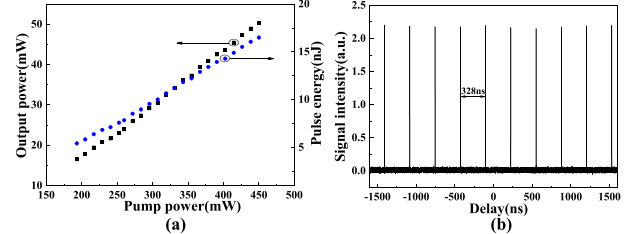


Fig. 2. (a) The average output power (black) and the single-pulse energy (blue) for different pump power. (b) Output pulse trains.

counter-pumped by a 976 nm laser diode (Oclaro LC96U, a maximum power of 680 mW) through the WDM. The NPE in the cavity is optimized by a half waveplate and other two quarter waveplates. The length and GVD of all fibers within the cavity are summarized in Table 1. The total length of the fiber is 65.5 m and the optical path of free-space region within the cavity is 25 cm, resulting in a ~ 3.05 MHz fundamental repetition rate. Considering the GVD of the isolator ($\sim 0.003\text{ps}^2$), the SESAM ($\sim 0.003\text{ps}^2$) and other free-space bulk components ($\sim -0.0005\text{ps}^2$), the net GVD of the whole cavity is estimated to be $\sim 1.28 \text{ ps}^2$ at the central wavelength of 1550 nm. It is noted that no additional spectral filter is inserted into the laser cavity, and the stabilization of the mode-locking is dominated by the limited gain bandwidth of the Er-doped gain fiber.

The laser output is characterized by an autocorrelator (Femtochrome, FR-103XL) and an optical spectrum analyzer (Yokogawa AQ6370C). The pulse train and RF spectrum are detected by a 16 GHz photodetector (Discovery Semiconductor DSC720), and then analyzed by a 2.5 GHz oscilloscope (Agilent DSO9254A) and a signal source analyzer (R&S FSUP50).

III. RESULTS AND DISCUSSION

Figure 2 (a) shows the dependence of the laser's average output power and single-pulse energy on the pump power. At the threshold pump power of 193 mW, mode-locking of the laser is easily achieved by adjusting the wave plates. After mode-locking, the laser generates stable pulse trains with a period of about 328 ns; the fundamental repetition rate is thereby around 3.05 MHz, which agrees well with that expected from the 65.5 m-long cavity. When the pump power is in the range of 193 to 450 mW, the proposed hybrid mode-locking fiber laser operates on the single-pulse state, and the single pulse operation is self-starting and highly stable which can continuously operate over 48 hours. At the pump power of 450 mW, the average output power of the mode-locking pulses is 50.31 mW, indicating an overall efficiency of 11.2%. The maximum single-pulse energy of the hybrid mode-locking fiber laser is estimated to be 16.5 nJ. Figure 2 (b) shows

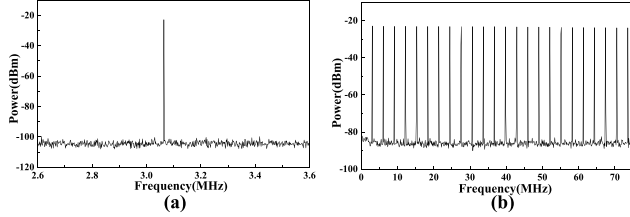


Fig. 3. (a) RF spectrum of fundamental mode beat measured at a 300 Hz resolution bandwidth, (b) RF spectrum of harmonics with a 75 MHz span measured at a 10 kHz resolution bandwidth.

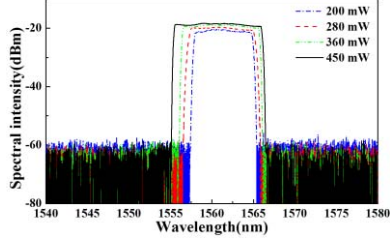


Fig. 4. Evolution of the output spectrum as the pump power is tuned from 200 mW to 450 mW.

equally spaced pulses emitted from the laser, suggesting no signs of dual-pulsing or Q-switched mode-locking operation of laser oscillator. The slight fluctuation in pulse amplitude can be attributed to the insufficient bandwidth and resolution of the oscilloscope. The RF spectrum of the fundamental mode beat is illustrated in Fig. 3(a). The signal-to-background ratio of the fundamental frequency is up to 80 dB at a resolution bandwidth of 300 Hz, and no sideband is observed within a frequency range of 1 MHz. Figure 3(b) presents the RF spectrum up to a frequency of 75 MHz at a resolution of 10 kHz, which further verifies the high stability of our hybrid mode-locked Er-doped fiber laser. The relative intensity noise (RIN) can be estimated by adopting the von der Linde's method. For a noisy pulse train after the photodetector, the RIN is derived as [24]:

$$\begin{aligned} RIN &= \left(\frac{\Delta I}{I} \right)^2 \\ &= 2 \int_0^{\frac{f_R}{2}} \left[R_1/f_{res} - \left(\frac{R_{10}(f) - R_1(f)}{99 f_{res}} \right) \right] df \end{aligned}$$

Where f_R is the fundamental repetition rate, $R_k(f)$ is the relative value in k^{th} component with respect to offset frequency ($f = f_i - kf_{res}$), k is the harmonic number, f_{res} is the resolution bandwidth of the RF spectrum. The calculated RIN of our fiber laser is 0.054% integrated from 1 kHz to 1.525 MHz. This agrees with the measurements of other dissipative solitons fiber laser [25] and validates the accuracy of the described RIN estimate. When the pump power is more than ~ 450 mW, the fiber laser operates on the multi-pulse state. In the experiment, we replaced the SESAM with another one which presents a modulation depth of 24%, a recovery time of 2 ps, and a saturation fluence of $70 \mu\text{J}/\text{cm}^2$. But the hybrid mode-locked lasers are relatively unstable due to larger absorbance loss (40%), and there is no increase in pulse energy.

Figure 4 depicts the optical spectrum at different pump power with a spectrum resolution of 0.02 nm. When the pump power is increased from 200 mW to 450 mW, the full

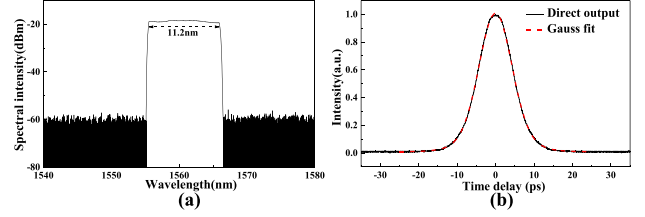


Fig. 5. Experimental results at a pump power of 450 mW. (a) Optical spectrum measured by OSA. (b) The autocorrelation trace of the direct output pulse (black solid curve) and its Gaussian fit (red dash curve).

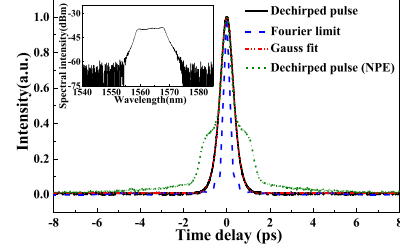


Fig. 6. The autocorrelation trace of the compressed pulse (black solid curve). The blue dash curve is the Fourier transform of spectrum. The inset is the optical spectrum of the NPE-based mode-locking.

spectrum width at half maximum (FWHM) of the output spectrum is broadened from 7.2 nm to 11.2 nm and the center wavelength slightly shifts toward the short-wavelength direction. The physical reason is attributed to the fact that the power stored in the laser cavity is increased and the induced nonlinear effects in the fiber become strong. When the pump power is maintained at 450 mW, the optical spectrum and the autocorrelation trace of the direct output pulses are shown in Fig. 5(a) and Fig. 5(b), respectively. The optical spectrum of the mode-locking pulses has the characteristic of steep spectral edges, indicating that the generated pulses are DSs and the mode-locked fiber lasers operate in the large positive dispersion regime. The FWHM of the output spectrum is 11.2 nm (from ~ 1555.12 nm to ~ 1666.32 nm) centered at 1560.72 nm and its shape is a rectangle. It is noted that no apparent concavity emerges in the top flatness of the optical spectrum, and there is no pedestals existing on both sides of the spectrum. In addition, the dependence of the rectangular shape on waveplates orientation is also investigated to further optimize the laser output characteristics. Although some changes such as spectrum width and intensity are observed in the spectral waveform, but the rectangular shape is maintained with negligible variation. Figure 5(b) shows the autocorrelation trace of the direct output pulse with a width of 10.72 ps, corresponding to a pulse duration of 7.6 ps for Gaussian profile approximation. The calculated time-bandwidth product is 10.64, indicating that the output pulse has strong chirp due to large normal dispersion within the cavity. It should be noted that further lengthening the cavity by employing DCFs or SMF28e cannot enhance the pulse energy because the overdriving of the effective saturable absorber and pulse-breaking will arise.

Figure 6 shows the autocorrelation trace of the compressed pulse using a pair of transmission gratings with 966 lines/mm and 87.3% compressor efficiency external to the cavity, which has the minimum duration of 725 fs, corresponding to a pulse duration of 514 fs for Gaussian profile approximation.

The theoretical limit calculated by Fourier transformation of the optical spectrum (blue dash curve) is also plotted in comparison with the experimental compressed pulses. The compressed pulse is 17% higher than the Fourier transform limit of 441 fs, which indicates that there are some residual chirp induced by fiber nonlinearity and third-order dispersion. The pulse energy concentrated on the main peak is quantitatively assessed by integrating the pulse power from the peak to the side of a single pulse. It is noted that no apparent pedestal beats or satellite pulses can be observed in both sides of the DSs pulses, and the main peak contains more than 99% of the pulse energy, whereas this value is less than 80% in most other DSs lasers [22], [19]–[21], [23]. For comparison, the laser is just operated in NPE-based mode-locking when the SESAM is replaced by a highly reflective mirror. In this case, the autocorrelation trace of the compressed pulse is also shown in Fig. 6 (green short dash curve), which combines with large temporal beat pedestals containing more than 45% of the pulse energy. The corresponding spectrum is also shown in the inset of Figure 6 with a FWHM of about 10.2 nm. It is noted that the edge of the spectrum is less steep than that of hybrid mode-locking, which is due to the temporal beat pedestals exist in both sides of the pulses. Therefore, the hybrid mode-locking offers purified femtosecond pulses with high energy concentration, indicating that temporal beat pedestals are successfully suppressed by nonlinear amplitude modulation in the cavity with the assistance of the SESAM. The average output power of the compressed pulse is 43.92 mW, and the pulse peak power is estimated to be $P_{pk} = 26.1 \text{ kW}$ using $P_{pk} = 2\frac{W}{T}\sqrt{\ln(2)\pi}$, where W is pulse energy and T is the pulse duration [26]. In addition to high-power applications, these laser characteristics are also beneficial to construct a fiber-based comb that requires efficient nonlinear spectral broadening and second-harmonic generation for a self-referenced f-2f interferometer [27].

IV. CONCLUSION

In conclusion, we have demonstrated a hybrid mode-locked Er-doped fiber laser capable of generating 16.5 nJ single-pulse energy and 26.1 kW pulse peak power with a repetition rate of 3.05 MHz. The laser delivers an average output power of 50.32 mW at a pump power of 450 mW, corresponding to an overall efficiency of 11.2%. The FWHM of the optical spectrum is 11.2 nm and the pulse duration of the compressed pulse is 514 fs. No apparent pedestal beats or satellite pulses is observed in both sides of the time domain pulse. The mode-locking is self-starting and stable over 48 hours. However, there are still a lot of work to be undertaken in future. For example, the evolution of pulse spectral and temporal parameters along the cavity are important to fully reflect the overall performance of the laser. Therefore, numerical simulation is important to guide future experiments.

REFERENCES

- [1] C. Jauregui, J. Limpert, and A. Tünnermann, "High-power fibre lasers," *Nature Photon.*, vol. 7, pp. 861–867, Oct. 2013.
- [2] Y.-Y. Zhang *et al.*, "High-energy subpicosecond pulse generation from a mode-locked Yb-doped large-mode-area photonic crystal fiber laser with fiber facet output," *IEEE Photon. Technol. Lett.*, vol. 22, no. 5, pp. 350–352, Mar. 1, 2010.
- [3] F. W. Wise, A. Chong, and W. H. Renninger, "High-energy femtosecond fiber lasers based on pulse propagation at normal dispersion," *Laser Photon. Rev.*, vol. 2, nos. 1–2, pp. 58–73, 2008.
- [4] I. N. Duling, "All-fiber ring soliton laser mode locked with a nonlinear mirror," *Opt. Lett.*, vol. 16, no. 8, pp. 539–541, 1991.
- [5] K. Tamura, E. P. Ippen, H. A. Haus, and L. E. Nelson, "77-fs pulse generation from a stretched-pulse mode-locked all-fiber ring laser," *Opt. Lett.*, vol. 18, no. 13, pp. 1080–1082, 1993.
- [6] F. Ö. Ilday, J. R. Buckley, W. G. Clark, and F. W. Wise, "Self-similar evolution of parabolic pulses in a laser," *Phys. Rev. Lett.*, vol. 92, p. 213902, May 2004.
- [7] A. Chong, J. Buckley, W. Renninger, and F. Wise, "All-normal-dispersion femtosecond fiber laser," *Opt. Exp.*, vol. 14, no. 21, pp. 10095–10100, 2006.
- [8] M. Guina, N. Xiang, A. Vainionpää, O. G. Okhotnikov, T. Sajavaara, and J. Keinonen, "Self-starting stretched-pulse fiber laser mode locked and stabilized with slow and fast semiconductor saturable absorbers," *Opt. Lett.*, vol. 26, no. 22, pp. 1809–1811, 2001.
- [9] H. Liu, Z. Liu, E. S. Lamb, and F. Wise, "Self-similar erbium-doped fiber laser with large normal dispersion," *Opt. Lett.*, vol. 39, no. 4, pp. 1019–1021, 2014.
- [10] B. Ortaç, M. Baumgartl, J. Limpert, and A. Tünnermann, "Approaching microjoule-level pulse energy with mode-locked femtosecond fiber lasers," *Opt. Lett.*, vol. 34, no. 10, pp. 1585–1587, 2009.
- [11] J. An, D. Kim, J. W. Dawson, M. J. Messerly, and C. P. J. Barty, "Grating-less, fiber-based oscillator that generates 25 nJ pulses at 80 MHz, compressible to 150 fs," *Opt. Lett.*, vol. 32, no. 14, pp. 2010–2012, 2007.
- [12] C. Lecaplain, C. Chédot, A. Hideur, B. Ortaç, and J. Limpert, "High-power all-normal-dispersion femtosecond pulse generation from a Yb-doped large-mode-area microstructure fiber laser," *Opt. Lett.*, vol. 32, no. 18, pp. 2738–2740, 2007.
- [13] F. Ö. Ilday, J. R. Buckley, H. Lim, F. W. Wise, and W. G. Clark, "Generation of 50-fs, 5-nJ pulses at 1.03 μm from a wave-breaking-free fiber laser," *Opt. Lett.*, vol. 28, no. 15, pp. 1365–1367, 2007.
- [14] A. Chong, W. H. Renninger, and F. W. Wise, "All-normal-dispersion femtosecond fiber laser with pulse energy above 20 nJ," *Opt. Lett.*, vol. 32, no. 16, pp. 2408–2410, 2007.
- [15] N. B. Chichkov, K. Hausmann, D. Wandt, U. Morgner, J. Neumann, and D. Kracht, "High-power dissipative solitons from an all-normal dispersion erbium fiber oscillator," *Opt. Lett.*, vol. 35, no. 16, pp. 2807–2809, 2010.
- [16] A. Cabasse, D. Gaponov, K. Nda, A. Khadour, J.-L. Oudar, and G. Martel, "130 mW average power, 4.6 nJ pulse energy, 10.2 ps pulse duration from an Er³⁺ fiber oscillator passively mode locked by a resonant saturable absorber mirror," *Opt. Lett.*, vol. 36, no. 14, pp. 2620–2622, 2011.
- [17] M. Tang *et al.*, "High-energy dissipative solitons generation from a large normal dispersion Er-fiber laser," *Opt. Lett.*, vol. 40, no. 7, pp. 1414–1417, 2015.
- [18] A. Ruehl, V. Kuhn, D. Wandt, and D. Kracht, "Normal dispersion erbium-doped fiber laser with pulse energies above 10 nJ," *Opt. Exp.*, vol. 16, no. 5, pp. 3130–3135, 2008.
- [19] X. M. Liu and D. Mao, "Compact all-fiber high-energy fiber laser with sub-300-fs duration," *Opt. Exp.*, vol. 18, no. 9, pp. 8847–8852, 2010.
- [20] C. Ouyang *et al.*, "Dissipative soliton (12 nJ) from an all-fiber passively mode-locked laser with large normal dispersion," *IEEE Photon. J.*, vol. 3, no. 5, pp. 881–887, Oct. 2011.
- [21] J. Peng *et al.*, "Direct generation of 4.6-nJ 78.9-fs dissipative solitons in an all-fiber net-normal-dispersion Er-doped laser," *IEEE Photon. Technol. Lett.*, vol. 24, no. 2, pp. 98–100, Jan. 15, 2012.
- [22] N. B. Chichkov, K. Hausmann, D. Wandt, U. Morgner, J. Neumann, and D. Kracht, "50 fs pulses from an all-normal dispersion erbium fiber oscillator," *Opt. Lett.*, vol. 35, no. 18, pp. 3081–3083, 2010.
- [23] A. Cabasse, G. Martel, and J. L. Oudar, "High power dissipative soliton in an erbium-doped fiber laser mode-locked with a high modulation depth saturable absorber mirror," *Opt. Exp.*, vol. 17, no. 12, pp. 9537–9542, 2009.
- [24] D. von der Linde, "Characterization of the noise in continuously operating mode-locked lasers," *Appl. Phys. B, Condens. Matter*, vol. 39, no. 4, pp. 201–217, 1986.
- [25] I. L. Budunoğlu, C. Ülgür, B. Oktem, and F. Ö. Ilday, "Intensity noise of mode-locked fiber lasers," *Opt. Lett.*, vol. 34, no. 16, pp. 2516–2518, 2009.
- [26] X. Li, W. Zou, G. Yang, and J. Chen, "Direct generation of 148 nm and 44.6 fs pulses in an erbium-doped fiber laser," *IEEE Photon. Technol. Lett.*, vol. 27, no. 1, pp. 93–96, Jan. 1, 2015.
- [27] S. Kim *et al.*, "Hybrid mode-locked Er-doped fiber femtosecond oscillator with 156 mW output power," *Opt. Exp.*, vol. 20, no. 14, pp. 15054–15060, 2012.